Current Research in Food Science 1 (2019) 31–42

Contents lists available at ScienceDirect

Current Research in Food Science

journal homepage: www.editorialmanager.com/crfs/

Research Paper

Effect of cysteine addition and heat treatment on the properties and microstructure of a calcium-induced whey protein cold-set gel

Anaïs Lavoisier [a,b,*], Thomas A. Vilgis [b], José Miguel Aguilera [a]

[a] Department of Chemical and Bioprocess Engineering, Pontificia Universidad Católica de Chile, Av. Vicuña Mackenna, 4860, Macul, Santiago, Chile
[b] Max Planck Institute for Polymer Research, Ackermannweg 10, 55128, Mainz, Germany

ARTICLE INFO

Keywords:
Protein network
Cold gelation
Fractal dimension
Atomic force microscopy
Cryo-SEM
Rheology

ABSTRACT

A model gel of whey protein isolate (WPI) was prepared by cold gelation with calcium. This system was modified by the addition of free cysteine residues (Cys) at different steps of the process. The WPI cold-set gels obtained were then subjected to heat treatment at 90°C. First, the effect of Cys addition on the heat-induced aggregation of WPI was studied through Atomic Force Microscopy (AFM) and infrared spectroscopy (ATR-FTIR), while Cys' effect on cold gelation was observed by AFM, Confocal Laser Scanning Microscopy (CLSM) and oscillatory rheology (amplitude sweeps). The impact of heating on the microstructure and the viscoelastic properties of the WPI cold-set gels were finally investigated through several techniques, including DSC, ATR-FTIR, CLSM, cryo-SEM, and rheological measurements (temperature sweeps). When added during the first step of cold gelation, Cys modified heat-induced aggregation of WPI, resulting in the formation of a denser gel network with a fractal dimension (Df) of 2.8. However, the addition of Cys during the second step of cold gelation led to the formation of highly branched clusters of WPI and a looser gel network was observed (Df = 2.4). In this regard, the use and limitations of oscillatory rheology and the "Kraus model" to determine the Df of WPI cold-set gels was discussed. The viscoelastic properties and the microstructure of the WPI cold-set gels were irreversibly modified by heating. Gels were stiffer, more brittle, and coarser after heat treatment. New disulfide bonds and calcium bridges formed, as well as H-bonded β-sheets, all contributing to the formation of the final gel network structure.

1. Introduction

Whey proteins are by-products of cheese manufacture used as functional foods in sports nutrition, as dietary supplements for the elderly and as functional ingredients for the food industry (e.g., in emulsions, foams, gels and fat reduced products) (Smithers, 2015).

The main components of whey proteins in bovine milk are the globular proteins β-lactoglobulin (β-lg) which represents more than 50% of the total proteins, α-lactalbumin (α-la) ca. 20%, and bovine serum albumin (BSA). The gelling properties of whey proteins are mainly related to the β-lg (Havea et al., 2001), but α-la and BSA are also involved in gelation (Hines and Foegeding, 1993).

Native β-lg is made of a sequence of 178 amino acids, including a signal peptide of 16 residues, and contains seven cysteine residues. Two of them are on the signal peptide, four others form disulfide bridges, between Cys^{82} and Cys^{176} (near the C-terminus) and between Cys^{122} and Cys^{135} (in the interior of the molecule), while the last one, Cys^{137}, is a free thiol group (The UniProt Consortium, 2019). The secondary structure of β-lg consists of about 8% α-helix, 45% β-sheet and 47% random coil. This structure is organized as strands of anti-parallel β-sheet and forms a hydrophobic barrel (The UniProt Consortium, 2019). At room temperature and neutral pH, native β-lg exists as a dimer of two non-covalently linked monomeric molecules.

Upon heating, dimer dissociation occurs first (between 30 and 55 °C), followed by reversible partial unfolding (above 60 °C) (Cheison and Kulozik, 2017). In this molten globule state, the free thiol group and part of the hydrophobic groups that were previously buried inside the globular structure are exposed and therefore available for reaction (Bryant and McClements, 1998). Further heating leads to irreversible aggregation of β-lg, mainly through intermolecular disulfide cross-linking (Hoffmann and Van Mil, 1997). Hydrophobic non-covalent interactions are also involved in heat-induced aggregation of β-lg and seem to contribute to the stabilization of the protein aggregates after cooling (Nguyen et al., 2014).

Whey proteins are known to form gels by heating dispersions over 70

* Corresponding author. Department of Chemical and Bioprocess Engineering, Pontificia Universidad Católica de Chile, Av. Vicuña Mackenna, 4860, Macul, Santiago, Chile.
E-mail address: alavoisier1@uc.cl.edu (A. Lavoisier).

https://doi.org/10.1016/j.crfs.2019.10.001

°C and above a critical protein concentration (Aguilera, 1995). Through controlled heat-treatment, stable soluble aggregates of whey protein can be formed. Their morphology and size vary with pH, ionic strength, type of salt and protein concentration (Nicolai and Durand, 2013). At pH 7 and low ionic strength, whey protein heat-induced aggregates are described as flexible strands (Jung et al., 2008) that subsequently associate into larger randomly branched aggregates (or flocs) when the protein concentration is increased (Ikeda and Morris, 2002). Gelation can then be induced by reducing the electrostatic repulsion between the whey protein aggregates, either by adding a salt like NaCl or $CaCl_2$ (Kharlamova et al., 2018a; Marangoni et al., 2000) or by decreasing the pH (Kharlamova et al., 2018b; Alting et al., 2002). This two-step process – heat-induced aggregation followed by association of aggregates at ambient temperature – is known as cold gelation.

In cold gelation induced by $CaCl_2$, calcium divalent cations connect different protein chains at their negatively charged amino acids, whenever the created meshes have sufficient size and entropy (i.e., the distance between the possible binding sites is large enough), and form calcium bridges between the heat-induced aggregates of whey proteins (Bryant and McClements, 2000). This method leads to the formation of a particle gel network of fractal nature (Marangoni et al., 2000; Walstra et al., 1991; Andoyo et al., 2018; Hongsprabhas, 1997; Hongsprabhas and Barbut, 1997a). The effect of salt type and concentration, protein concentration, size and shape of the aggregates, temperature, etc., on the microstructure of the network and the properties of whey protein gels prepared by cold gelation has been extensively studied (Kharlamova et al., 2018a; Brodkorb et al., 2016). However, little is known about changes induced by additional heat treatment on cold-set whey protein gels, although heating is common during cooking, industrial food processing and pasteurization. Moreover, heating generally influences the functional and viscoelastic properties of foods, and therefore, it seems to be a critical parameter to consider in the formulation of new food products. Hongsprabhas and Barbut (1997b) reported that when cold-set whey proteins gels induced by calcium were heated at 80 °C for 30 min, the opacity, fracture properties and water holding capacity of the final gels were modified. They suggested that these changes in the characteristics of the gels were related to further aggregation of the proteins during heating, either through hydrophobic interactions or chemical reactions. Similarly, in previous work on composite cold-set gels made of whey proteins and potato starch, we observed that the rheological and mechanical properties of the protein gel were altered by heat treatment above 85 °C (Lavoisier and Aguilera, 2019).

L-Cysteine (Cys) is a non-essential amino acid, with a thiol side chain susceptible to oxidation. It is a food-grade additive, often added to wheat flour to aid dough development and improve the quality of baked products (Majzoobi et al., 2011; Elkhalifa and El-Tinay, 2002). Cys acts mainly as a free thiol group blocking reagent, similar to N-ethylmaleimide (NEM), but Cys may also cleave intramolecular disulfide bonds in proteins (Huggins et al., 1951; Wang and Damodaran, 1990). Cys is capable of interfering with the thiol-disulfide interchange reaction during heat treatment of globular proteins (Dan and Labuza, 2010). The effect of Cys on the properties of heat-set whey protein gels seems to depend on the quantity added: moderate Cys addition increase gel strength, while higher concentrations of added Cys reduce gel strength (Wang and Damodaran, 1990; Dan and Labuza, 2010; Schmidt et al., 1978, 1979). To the best of our knowledge, the effect of Cys addition on cold gelation of whey proteins has not been systematically studied.

The objective of this study was two-fold. On the one hand, we investigated the effect of Cys addition on whey proteins' cold gelation. And on the other hand, we evaluated the impact of heat treatment on the properties and microstructure of whey protein cold-set gels. A model gel of whey protein isolate (WPI) was prepared by cold gelation with calcium, and free Cys residues were added at different steps of the process. The hypothesis of this work was that Cys addition and heating could modify the viscoelastic properties of whey protein cold-set gels through the alteration of the structure of the particle gel network.

2. Material & methods

2.1. Materials

BiPro® WPI with a moisture content of 4.6% and a protein content of 95% (d.b.) was purchased from Davisco (Davisco Foods International Inc., Le Sueur, MN, USA). According to the manufacturer, the protein content was divided as follow: 50% of β-lactoglobulin, 20% of α-lactalbumin and 30% of other proteins including bovine serum albumin. L-Cys 30089 BioUltra ≥98.5% (RT) was from Sigma-Aldrich (Sigma Chemical Co., St. Louis, MO, USA). All other chemicals were standard analytical grade and Milli-Q® water was used for the preparation of all mixtures.

2.2. Sample preparation

WPI gels were prepared by cold gelation induced by calcium chloride ($CaCl_2$) addition. First, a dispersion of 10% (w/w) WPI was prepared by stirring the WPI powder in water for 90 min at 600 rpm (pH of the dispersion = 7). This dispersion was then filtered (Minisart syringe filter, hydrophilic, pore size 0.2 μm from Sartorius Stedim Biotech GmbH, Goettingen, Germany) and heated in a circulating water bath at 80 °C for 30 min. Protein particles of at least 25 nm of hydrodynamic diameter were obtained (measured through dynamic light scattering, data not shown), meaning that all native WPI had aggregated during this first heating step. The sample was cooled to room temperature under running cold tap water for 5 min and 1 mL of a 100 mM $CaCl_2$ aqueous solution was dropped into 9 mL of the WPI dispersion while stirring at 600 rpm. This mixture was then immediately transferred to glass vials (5 mL) for cryo-SEM studies. To measure the thermal properties as well as in the case of ATR-FTIR and CLSM studies, 50 mg of the sample was sealed in a 100 μL aluminum pan. For rheological measurements, the sample was directly cast in a mold fixed on the lower rheometer plate (25 mm in diameter and 1 mm of height). All samples were finally stored overnight at 4 °C.

Free Cys were added at different steps of the cold gelation: before heat induced aggregation of WPI (i.e., before heating at 80 °C for 30 min), before cold gelation of the WPI aggregates (i.e., before $CaCl_2$ addition), or during cold gelation of the WPI aggregates (i.e., with $CaCl_2$ addition). In each case, the concentration of Cys added was 2.6 mM. This concentration was chosen to equal the calculated concentration of β-lactoglobulin molecules in the mixture in the experimental conditions described before.

2.3. Thermal properties

Samples gelled in the hermetically sealed pans were heated from 20 to 100 °C at 1 °C/min with a Mettler Toledo DSC 822 (Mettler-Toledo Inc., Columbus, OH, USA). A pan containing 50 mg of water was used as a reference and the equipment was calibrated with indium. Results were analyzed with the STARe Thermal Analysis Evaluation software, version 14.0 (Mettler-Toledo Inc., Columbus, OH, USA). Each measurement was done in triplicate.

2.4. Attenuated total reflectance Fourier-transformed infrared spectroscopy (ATR-FTIR)

Heat treatment of the gels was performed with the DSC instrument as described before (cf. Section 2.3). The aluminum lid was carefully removed and gel samples were extracted from the pan and directly measured. ATR-FTIR spectroscopy was performed using a Brucker Tensor II instrument, equipped with a Platinum ATR (Brucker Optik GmbH, Ettlingen, Germany). Data were acquired between 4000 and 400 cm^{-1} with a resolution of 4 cm^{-1} and averaging 32 scans for each spectrum. A

background spectrum was scanned at the beginning of the measurements using the same instrumental conditions as for the sample spectra acquisition, as well as a water spectrum and a control spectrum (unheated WPI in water). Samples were first equilibrated at room temperature for one hour. For liquid samples, one drop of the dispersion was added onto the ATR cell. For gels, samples were gently pressed onto the ATR cell by using the integrated pressure application device with a glass slide. The experiments were performed in duplicate.

The water spectrum was used as baseline and the spectrum of the control sample of unheated WPI in water was subtracted from the samples spectra. The study was focused on the Amide I absorption region (1700–1600 cm^{-1}) in order to investigate changes in the secondary structure of the whey proteins.

2.5. Rheological properties

For all rheological measurements, a TA Instruments Discovery Hybrid Rheometer HR-3 equipped with an advanced Peltier plate and a solvent trap and evaporation blocker (TA Instruments Corp., New Castle, DE, USA) was used. The solvent trap of the 40 mm top parallel plate was filled with distilled water and the gap size was 1 mm. Amplitude sweeps were performed at 20 °C at a constant frequency of 1 Hz, between 0.02 and 2000% strain (γ), measuring 20 points per decade. Sandpaper was used on both plates to avoid sample slipping under increasing strain amplitude. Temperature sweeps were carried out from 20 to 50, 60, 70, 80 or 90 °C and from 50, 60, 70, 80 or 90 to 20 °C with a heating/cooling rate of 1 °C/min, at a constant frequency of 1 Hz and a constant strain of 1.0%, which was in the linear viscoelastic region (LVR) for all samples. An axial force of compression of 0.5 N ± 0.1 N was used as conditioning to avoid losing contact between the plates and the sample during the test. After this oscillatory temperature ramp, gels were equilibrated for 15 min at 20 °C and subjected to an amplitude sweep test in order to measure the rheological properties of the gels after heat treatment. Each measurement was performed in triplicate. From amplitude sweep curves, the plateau value of G′ (G'_0) and tan δ were both evaluated at $\gamma = 0.01\%$. The critical strain, corresponding to the end of the LVR of the gels was defined as the value of γ for which G′ had dropped to 90% of G'_0. These parameters were evaluated for both amplitude sweep curves before and after heat treatment.

2.6. Isothermal Titration Calorimetry (ITC)

ITC experiments were carried out using a MicroCal PEAQ-ITC (Malvern Panalytical, Malvern, UK) with a 200 μL sample cell, a 40 μL titration syringe, 0.4–2.0 μL injection volumes and 150 s interval between injections. The temperature was set at 25 °C and the stirring rate at 750 rpm. Measurements were done in triplicate. A $CaCl_2$ solution (100 mM) was titrated into a Cys solution (5 mM). To correct the data by the heat of dilution, the titrant ($CaCl_2$ solution) was titrated into distilled water and the obtained heats were subtracted from the titration of Cys with $CaCl_2$. Raw ITC data are reported (differential power vs. time) where each spike represents the injection of titrant into the cell, as well as the integrated and normalized heat plotted vs. the molar ratio of $CaCl_2$ to Cys. Data were fit using the MicroCal PEAQ-ITC instrument control software ("One Set of Sites" binding model).

2.7. Atomic Force Microscopy

For AFM observations, the samples were diluted after heating at 80 °C for 30 min to reach a final protein concentration of $\sim 5.10^{-3}$ μg/mL, before adding $CaCl_2$ and/or Cys. The solutions of $CaCl_2$ and Cys were diluted accordingly, to maintain the ratios of calcium ions to protein and Cys to protein detailed previously (cf. Section 2.2). Then, a 10 μL drop of the sample was deposited onto the surface of a freshly cleaved mica phlogopite disk. For the observation of the unheated WPI in water, the sample was dried with a gentle blow of argon gas after one minute of incubation. For the observation of the other samples, mica disks were first preheated at 70 °C in an oven and samples were then air dried in the same oven at 70 °C for 5 min. AFM images were obtained with a Park NX20 instrument (Park Systems Corp., Suwon, South Korea) in tapping mode in air. Standard tapping mode AFM cantilevers with Al reflective coating were used (OPUS 160AC-NA, NanoAndMore GmbH, Wetzlar, Germany). Two replicates were prepared and observed for each experimental condition. Images were flattened and horizontal scars were corrected with the open source software Gwyddion (Nečas and Klapetek, 2012). AFM images of fractal aggregates and clusters were binarized with the open source ImageJ software (Schneider et al., 2012) and the D_f of each aggregate was analyzed with the fractal box count tool of the software (box sizes 2,3,4,6,8,12,16,32,64 and black background).

2.8. Confocal Laser Scanning Microscopy (CLSM)

As described previously, heat treatment of the gels was performed with the DSC instrument (cf. Section 2.3), the lids of the DSC pans were peeled and gels were carefully removed from the pans. A 10 μL drop of Rhodamine B (diluted in water at 0.001%) was placed in the well of a chambered coverglass and the gel sample was positioned on top of this staining drop. Gels were observed with a Zeiss LSM 880 inverted confocal laser scanning microscope (Carl Zeiss AG, Oberkochen, Germany) with an excitation wavelength of 543 nm. Fluorescence was measured at 565–600 nm and images were acquired with a water immersion objective C-Apochromat 40x/1.2 W (Carl Zeiss AG, Oberkochen, Germany). Three replicates were prepared and observed for each experimental condition. The open source ImageJ software and the image processing package Fiji were used to visualize and process the images (Schindelin et al., 2012). Image processing was the same for all samples: a "despeckle" filter was used first, then contrast was enhanced (saturated pixels 5%) and finally outliers were removed (radius 2 pixels, threshold 50, bright outliers). Processed images were binarized and areas where clear aggregates were visible were selected. D_f of each selected area was determined with the fractal box count tool of the software (box sizes 2,3,4,6,8,12,16,32,64 and black background).

2.9. Cryo-SEM

Gelled samples were heated inside the hermetically sealed glass vials at 90 °C for 30 min in a water bath and cooled in iced water for 5 min. Then, the microstructure of the gels before and after heat treatment were investigated with cryo-SEM, according to Ong, Dagastine, Kentish, and Gras (Ong et al., 2011) with modifications. A Hitachi SU8000 scanning electron microscope, equipped with a cryo-preparation system and a vacuum transfer device, was used (Hitachi Ltd, Tokyo, Japan). A piece of the gel was mounted on a copper holder and immersed into a freshly prepared nitrogen slush for 15 s. The frozen sample was then immediately transferred into the cryo-preparation chamber using the vacuum transfer device. The sample was fractured using a chilled scalpel blade in the chamber which was maintained at −120 °C under a high vacuum condition. The sample was then etched at −90 °C for 30 min. No coating was used. Finally, the sample was transferred under vacuum onto a nitrogen gas cooled module, maintained at −110 °C and observed at 2.0 kV. Two replicates were prepared and observed for each experimental condition.

3. Results and discussion

3.1. Effect of cysteine addition on the heat-induced aggregation of whey proteins

Fig. 1 shows the changes in the secondary structure of whey proteins after heating at 80 °C for 30 min in water at pH 7 determined by ATR-FTIR spectroscopy. Band intensity decreased at 1658 and 1630 cm^{-1}, wavelengths associated with α-helices and intramolecular β-sheets,

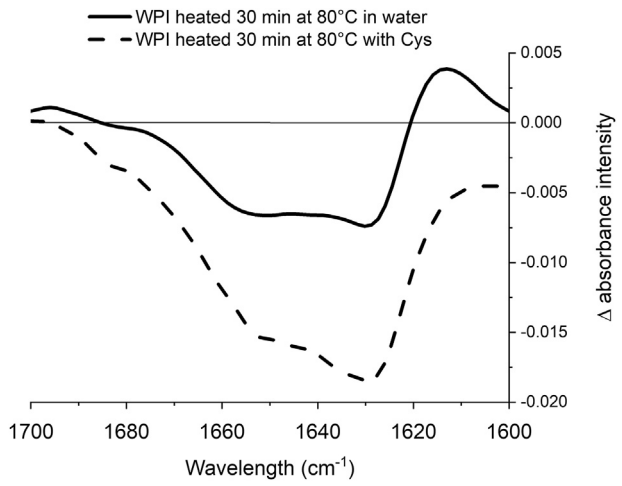

Fig. 1. ATR-FTIR spectroscopy spectra of WPI heated 30 min at 80 °C in water at pH 7 (solid line) and WPI heated 30 min at 80 °C in water at pH 7 with Cys (dash line). Both curves are subtracted from the unheated control of WPI.

respectively (Grewal et al., 2018), and increased at 1615 cm^{-1}, a wavelength associated to intermolecular β-sheets (Geara, 1999; Lefèvre and Subirade, 1999; Maltais et al., 2008). Therefore, the heat treatment resulted in interactions between the whey protein molecules, along with a partial loss of their intramolecular structure. Similar changes in the secondary structure of whey proteins were observed by O'Loughlin, Kelly, Murray, Fitzgerald, and Brodkorb (O'Loughlin et al., 2015) in BiPro® WPI dispersions (10% w/v) heated from 70 to 90 °C in water at pH 7. They suggested that the intermolecular interactions formed upon heating occurred through hydrophobic bonding at the β-lg dimer surface (I strand; His^{146}-Ser^{150}).

When Cys were added to the system, a steeper decrease in band intensity at 1658 and 1630 cm-1 was observed (Fig. 1), meaning that Cys caused a more significant loss in intramolecular structures. Cys may indeed cleave intramolecular disulfide bonds and therefore enhance the unfolding of proteins (Huggins et al., 1951; Wang and Damodaran, 1990). Then, the intensity of the band related to intermolecular β-sheets (ca. 1615 cm^{-1}) did not increase (Fig. 1), showing that less intermolecular interactions were formed during heating with Cys. This result was expected since Cys is capable of interfering with the thiol-disulfide interchange reaction during heat treatment of globular proteins (Dan and Labuza, 2010). When the free thiol group of β-lg is blocked by Cys, thermal unfolding is modified, and less hydrophobic sites are exposed and available to react, limiting intermolecular non-covalent interactions (Havea et al., 2009). So, ATR-FTIR spectroscopy demonstrated that Cys promoted the unfolding of whey proteins and hindered interactions between whey proteins during heating.

AFM was used to observe the effect of Cys on whey proteins at different stages of the cold gelation process (Fig. 2). Fig. 2a shows an image of the whey proteins before heat treatment. According to the height profiles of such AFM images, unheated whey proteins measured between 1 and 2.5 nm, which is in line with the literature (Ikeda and Morris, 2002; Elofsson et al., 1997; Kehoe et al., 2011). Fig. 2b shows the whey protein aggregates formed after heating at 80 °C for 30 min in water at pH 7. These aggregates had random shapes and measured ~3 μm in diameter. According to cryo-TEM studies, the β-lg pre-aggregates formed at pH 7 and low ionic strength have an elongated shape and measure less than 100 nm in length (Jung et al., 2008; Mahmoudi et al., 2007). But further association of these pre-aggregates may happen when protein concentration is increased up to 10% (w/w) (Durand et al., 2002). Therefore, the aggregates observed here were probably primary objects formed by smaller whey protein pre-aggregates.

In contrast, whey proteins heated with Cys formed irregular aggregates of ~0.3 μm in diameter (Fig. 2c). So, less protein molecules were able to interact with each other to form aggregates when Cys were added to the system. Since free Cys are able to react with Cys inside the whey proteins chains (Dan and Labuza, 2010), the free thiol groups of the β-lg (on the signal peptide and/or Cys^{137}) were probably blocked, and unable to form the thiol/disulfide exchange reactions responsible for the heat-induced aggregation of WPI (Hoffmann and Van Mil, 1997; Wijayanti et al., 2014; Wijayanti et al., 2013). However, regardless of the blocked thiol groups, the unfolded proteins may expose other active sites (e.g. hydrophobic regions) and still form aggregates via non-covalent interactions (Nguyen et al., 2014). It is therefore suggested that the aggregates observed in this case were mainly formed by non-covalent interactions.

These results indicate that heat-induced aggregation of whey proteins at pH 7 was modified by Cys addition. The presence of Cys in the system increased the unfolding of whey proteins and led to the production of smaller aggregates formed through non-covalent interactions such as hydrophobic interactions.

3.2. Effect of cysteine addition on cold gelation induced by calcium ions

3.2.1. Clusters

As shown in Fig. 2d and d', the addition of $CaCl_2$ at 20 °C to the dispersion of WPI aggregates (Fig. 2b) resulted in the formation of branched clusters with a mean diameter of ~11 μm. Calcium ions interacted with the whey protein aggregates and led to the formation of clusters with a fractal structure. Image analysis of the AFM pictures of these clusters yield a two-dimensional D_f of 1.84, which corresponds to the diffusion-limited cluster-cluster aggregation (DLCA) regime (Vreeker et al., 1992). Different values of D_f have been reported in the literature for WPI cold-set gels with $CaCl_2$ at pH 7. From the analysis of SEM images Kuhn, Cavallieri, and da Cunha (Kuhn et al., 2010) measured a D_f of 1.82 (in 2-D), while Marangoni, Barbut, McGauley, Marcone, and Narine (Marangoni et al., 2000), used TEM micrographs and obtained a higher D_f of 2.25. However, Hongsprabhas, Barbut, and Marangoni (Hongsprabhas et al., 1999) reported a $D_f = 1.5$ from the analysis of SEM and TEM micrographs. Finally, Wu, Xie, and Morbidelli (Wu et al., 2005) measured WPI clusters with a maximum average gyration radius of about 80 μm and a D_f of 1.85 ± 0.05 using small-angle light scattering. Besides the differences in the method used to determine D_f, the heat treatment as well as the protein and salt concentrations varied among these studies, which make them difficult to compare.

Calcium ions also interacted with the aggregates modified by Cys addition (cf. Fig. 2c), but the size and shape of the clusters formed were different (Fig. 2g and g'). Two main groups were distinguished: (1) branched clusters, mean size ~1.1 μm; and (2) unbranched clusters, mean size between 0.2 and 0.4 μm. According to Alting, Hamer, De Kruif, and Visschers (Alting et al., 2003), WPI clusters could be partly stabilized by the formation of additional covalent disulfide bonds. Therefore, it seems that the modified aggregates, where thiol groups were blocked, were not able to form these additional stabilizing bonds. Consequently, denser and smaller clusters (thermodynamically more stable than open branched clusters) were formed from WPI aggregates modified by Cys addition.

When Cys were added to the system after heat-induced aggregation of the whey proteins, the addition of $CaCl_2$ resulted in the formation of highly branched clusters, presented in Fig. 2e and e'. These clusters were heterogeneous in size, the larger ones measured ~17 μm in diameter and the smaller ones ~4 μm. Here, image analysis yield a Df of 1.75, which also corresponds to the DLCA regime, and confirms that these clusters had a more open structure than the unmodified WPI clusters (Fig. 2d and d'). Baussay, Le Bon, Nicolai, Durand, and Busnel (Baussay et al., 2004) observed that the density of β-lg aggregates on small length scales decreased when decreasing ionic strength. Here, Cys probably positioned themselves close to the surface of the aggregates and increased the steric hindrance around them. Consequently, interactions between the aggregates and the calcium ions were slowed, leading to the formation of loose clusters.

Interestingly though, when Cys were added at the same time as $CaCl_2$, the formation of clusters was clearly hindered, as shown in Fig. 2f and f'.

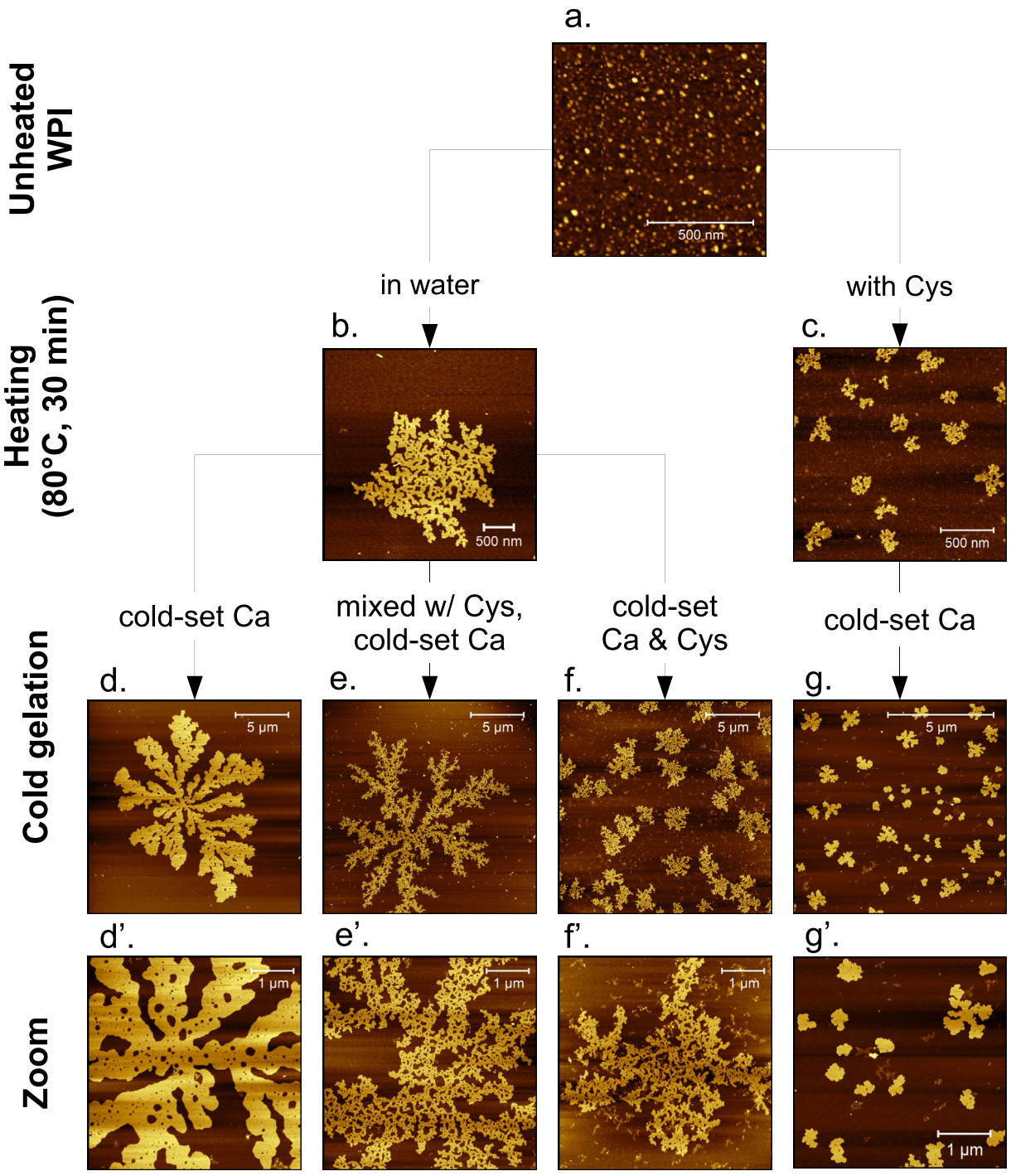

Fig. 2. Tapping mode AFM height images of (a) unheated WPI in water (pH 7), (b) WPI heated at 80 °C for 30 min in water, and (c) WPI heated at 80 °C for 30 min in water with free Cys; as well as clusters obtained by adding: (d and zoom d') calcium to the dispersion of WPI heat-induced aggregates; (e and zoom e') calcium to a dispersion of WPI heat-induced aggregates and free Cys; (f and zoom f') calcium and free Cys together in solution to the dispersion of WPI heat-induced aggregates; (g and zoom g') calcium to the dispersion of WPI heat-induced aggregates previously modified by heating with free Cys.

Small clusters of ~5 µm in diameter were observed, along with whey protein aggregates (~0.5 µm in diameter) that did not form clusters in spite of the addition of calcium to the system.

To understand this phenomenon better, complex formation between calcium ions and Cys in water at pH 7 was investigated with ITC. Fig. 3 shows the results of the titration of a $CaCl_2$ solution into a Cys solution. An endothermic transition with an association constant of ~5500 M^{-1} (ie., 1/KD) and a stoichiometric coefficient (N) around 1 was measured, suggesting that calcium and Cys did form complexes. Since this process was entropically driven, it is proposed that an ionic interaction occurred, excluding water molecules from the surface of Cys. Calcium ions probably interacted with the carboxyl group of Cys (ionized in water at pH 7). Therefore, the ionic strength of the solution was reduced when free Cys and calcium ions were dissolved together. Consequently, the conditions for cluster formation were significantly modified.

3.2.2. Gels

Amplitude sweep curves presented in Fig. 4 shows the effect of Cys addition on the viscoelastic properties of the calcium-induced cold-set gel. The four samples behaved as viscoelastic gels with dominating elastic

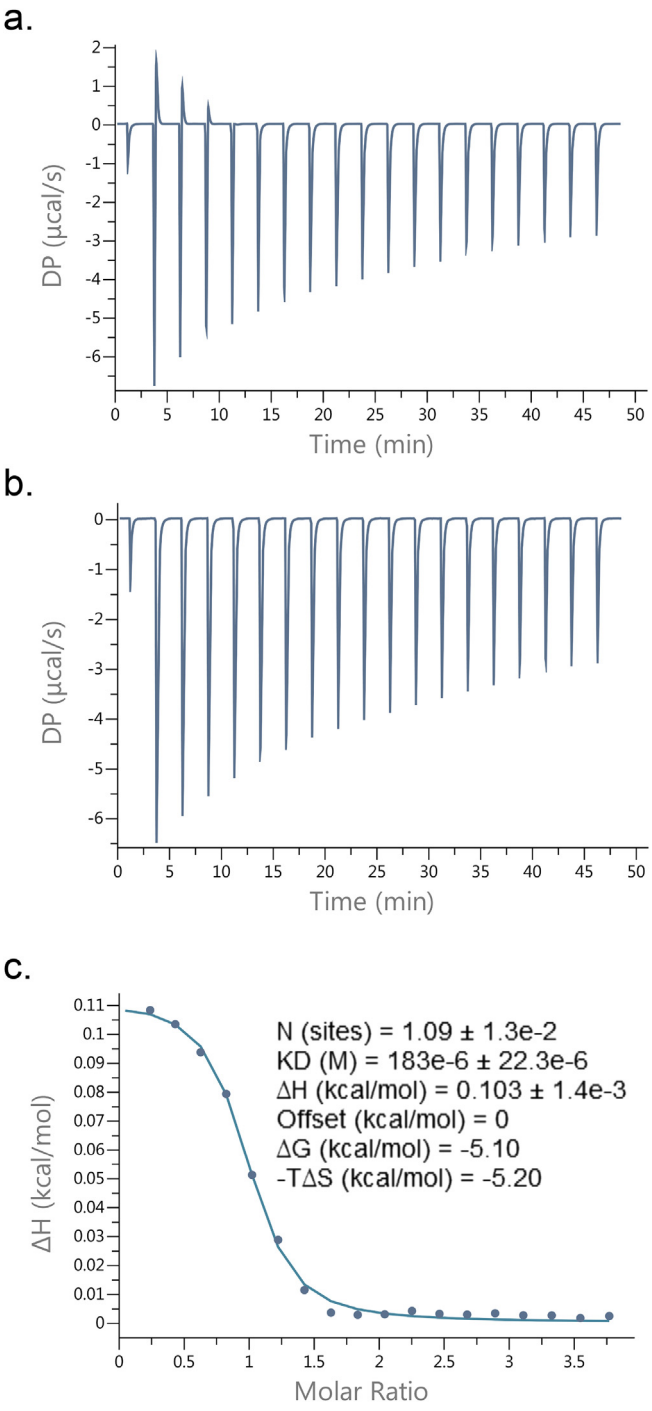

Fig. 3. Titration of 100 mM $CaCl_2$ into 5 mM Cys; (a) raw ITC data; (b) raw ITC data collected for the titration of 100 mM $CaCl_2$ into distilled water (= heat of dilution); (c) integrated and normalized heat vs. the molar ratio of $CaCl_2$ to Cys, after subtraction of the heat of dilution.

properties (tan δ < 1) in the LVR. The plateau value of G′ (called G'_0) was around 2 kPa for the calcium-induced cold-set gel (gel 1). Interestingly, from this experimental value of the shear modulus, it was possible to estimate the average number of bonds formed by calcium ions between the whey protein aggregates in this gel, as follow:

$$M_{agg} = \frac{M_{\beta-lg}}{\frac{number\ of\ protein\ molecules}{aggregates}} \quad (1)$$

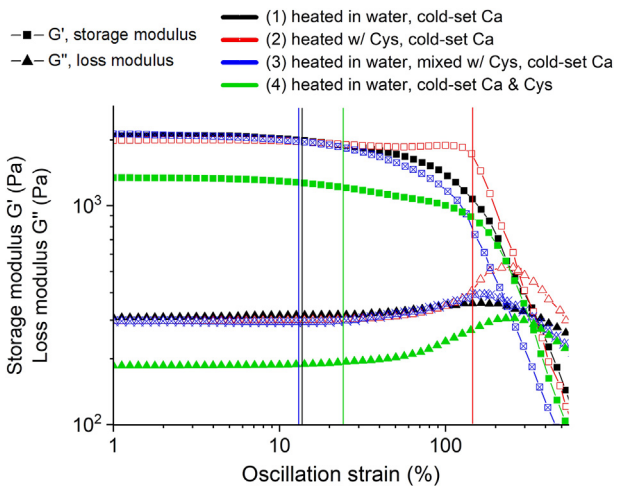

Fig. 4. Amplitude sweep curves of the four cold-set WPI gels: (1) WPI heated in water and cold-set with calcium; (2) WPI heated with Cys and cold-set with calcium; (3) WPI heated in water, mixed with Cys, and cold-set with calcium; (4) WPI heated in water, and cold-set with calcium and free Cys together in solution.

$$\frac{Number\ of\ bonds}{unit\ volume} = M_{\beta-lg} * \frac{number\ of\ bonds}{aggregates} \quad (2)$$

$$Total\ energy\ density = \frac{\frac{Number\ of\ bonds}{unit\ volume}}{E_{Ca^{2+}\&COO^-}} \quad (3)$$

where, M_{agg} is the molarity of β-lg aggregates in mol/L, $M_{\beta\text{-lg}}$ is the molarity of β-lg in mol/L in (1) and in mol/m^3 in (2), $E_{Ca2+\ \&\ COO-}$ is the bond energy of calcium ions with carboxyl groups in J/mol, and the total energy density is expressed in kPa.

This calculation was based on the following assumptions:

- the concentration in β-lg in the sample is 4.75% (w/w) and its' molecular weight is 18′600 g/mol,
- each aggregate is made of an average of 150′000 protein molecules (considering aggregates as squares on a plane with sides of ~2′000 nm, corresponding to ~400 protein molecules measuring ~5 nm; estimation based on the size of the aggregates observed on the AFM images, cf. Fig. 2b).
- the bond energy of calcium ions with carboxyl groups is ~77′000 J/mol (approximation based on the heat of formation of calcium formate (PSAAE, 2018)),

Based on these conditions, around 1′500 bonds per aggregates should be formed to reach a total energy density of 2 kPa in the system.

Adding Cys alone, during (gel 2) or after (gel 3) the formation of the whey protein aggregates, did not modified G'_0. But, when calcium and Cys were added together to the heat-induced aggregates (gel 4), G'_0 was significantly reduced to 1.3 ± 0.3 kPa (Fig. 4). This is consistent with the fact that less calcium ions were available to form salt bridges because of complex formation with Cys (cf. Fig. 3).

Under increasing shear amplitude, all samples showed a shear thinning behavior (Rao, 2007) probably due to the successive rupture of the links between the aggregates, until the complete destruction of the network (Fig. 4). Indeed, the elastic properties of whey protein networks formed by cold gelation induced by salts generally follow the weak-link regime (Andoyo et al., 2018). In the weak-link regime, the elastic behavior of the gels is dominated by the elastic constant of the interflocs links (ie., the calcium bridges), since the flocs (ie., the heat-induced aggregates) are more rigid than the interflocs links (Shih et al., 1990).

Irreversible deformation of samples occurred between 10 and 20% of oscillation strain, except when the heat-induced aggregates were modified by Cys (gel 2). In this case, the LVR of the gel was significantly increased as the breakdown of the network occurred at 144 ± 18% of oscillation strain (Fig. 4). A relationship exists between the structural properties of gels and their rheology (Roff and Foegeding, 1996). Different rheological properties were expected for gel 2 since it was formed from dense and small clusters united by non-covalent interactions (cf. AFM pictures, Fig. 2f and f'). It may be surmised that the lack of disulfide bonds allowed the proteins in the gel to rearrange when subjected to large deformation, extending the LVR, as proposed by Nguyen, Wong, Guyomarc'h, Havea, and Anema (Nguyen et al., 2014).

The observation through CLSM of the WPI network after cold gelation confirmed that significant differences existed between the microstructure of the gels 1 and 2 (Fig. 5). Both networks were homogeneous, but gel 1 had a typical mesh size of ~1.4 μm (Fig. 5a) while gel 2 had a significantly smaller mean mesh size of ~0.7 μm (Fig. 5b). Therefore, the modification of the whey protein aggregates by Cys during heating, further resulted in a denser gel network after calcium addition.

3.2.3. Fractal dimension of the gel

A D_f of 1.79 was yielded by the image analysis of CLSM pictures of the WPI cold-set gel with calcium (Fig. 5a), which is consistent with the Df of the WPI clusters determined by image analysis of AFM pictures (= 1.84, cf. Fig. 2d). However, the results obtained from the box counting method may depend on the threshold chosen during binarization (Ako et al., 2009) and theses values of the fractal dimension of the gel should be interpreted with caution.

Hence, the D_f of the WPI cold-set gels was also determined by oscillatory rheology. The rheological behavior of particle gels under deformation can be described by the "Payne effect" (Joshi et al., 2008); well-known from the elasticity of reinforced elastomers (see e.g. (Vilgis et al., 2009)), which can be quantified by applying the "Kraus model" on amplitude sweep curves. Amplitude sweep curves of the four WPI cold-set gels were therefore fitted with the following function:

$$G' = \frac{1}{1 + K^2 a^{2m}} \tag{4}$$

where G′ is the storage modulus (in Pa), K a constant depending on the system properties and a is the respective deformation amplitude (in %). The exponent m contains D_f as shown in Eq. (5):

$$m = \frac{1}{C - D_f + 2} \tag{5}$$

where C is the connectivity of the network. Here, C was set to 1.3 assuming that the WPI network is completely percolated (Joshi et al., 2008).

Results are shown in Fig. 6. The Kraus model suggested a $D_f = 2.42$ for the cold-set WPI gel with calcium (gel 1). Regardless of the method used to calculate D_f, the three-dimensional structure of WPI networks formed by calcium-induced cold gelation are generally described in the literature by D_f values around 2.6 (Andoyo et al., 2018). From rheological measurements, Hongsprabhas, Barbut, and Marangoni (Hongsprabhas et al., 1999), and Marangoni et al. (2000) reported a $D_f = 2.54$ for whey protein cold-set gels with $CaCl_2$, using the weak-link model developed by Shih, Shih, Kim, Liu, and Aksay (Shih et al., 1990). Kuhn et al. (2010) used the scaling model of Wu et al. (2005) for similar gels and reported a D_f of 2.66. In these studies, D_f was estimated from the values of the initial modulus G'_0 (in the linear deformation regime) of the gels measured at different WPI concentrations. In our work, D_f was calculated from the strain dependence of G′, considering the transmission of the stress in the network and the change of the internal structure of the gel. However, to understand the dependence of elasticity on the structure of the gels for larger, non-linear deformations, higher strains need to be taken into account, and for whey protein gels the rigid fractal model becomes invalid in the present form.

An overall shear thinning behavior under increasing shear amplitude could be described by the Payne effect, but additional effects were observed at high amplitudes, as can be seen in Fig. 6. Between 10 and 100% of oscillation strain, the Kraus model did not fit well the data. Especially for gel 2 and 4 where G′ decreased slowly, reached a plateau and finally dropped rapidly under increasing shear strain. In previous publications we applied the Kraus model to rigid fractals, corresponding to irregular particle gels, where primary particles were non deformable solids (Joshi et al., 2008; Vilgis et al., 2009). But here, the primary particles themselves are deformable. "Soft" fractals are formed, in which the individual WPI aggregates have their own elasticity and can deform before the entire network breaks down at larger shear amplitudes, as suggested by the amplitude sweep curves in Fig. 6. Thus, in contrast to particle gels formed by rigid fractals, the amplitude sweep curves of whey protein gels show a more complicated profile.

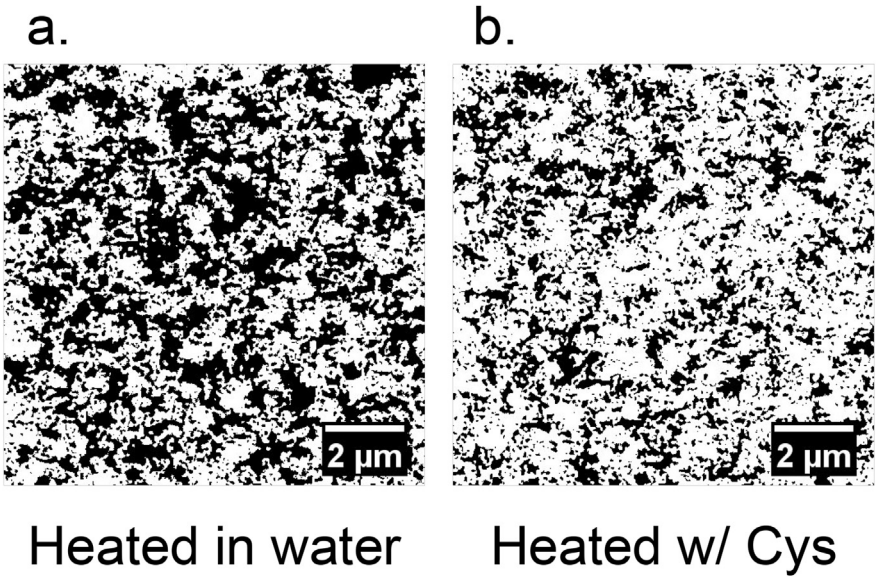

Fig. 5. CLSM images of the microstructure of the WPI network after cold gelation with calcium ions. (1) Calcium added to heat-induced aggregates; (2) calcium added to heat-induced aggregates modified by free Cys.

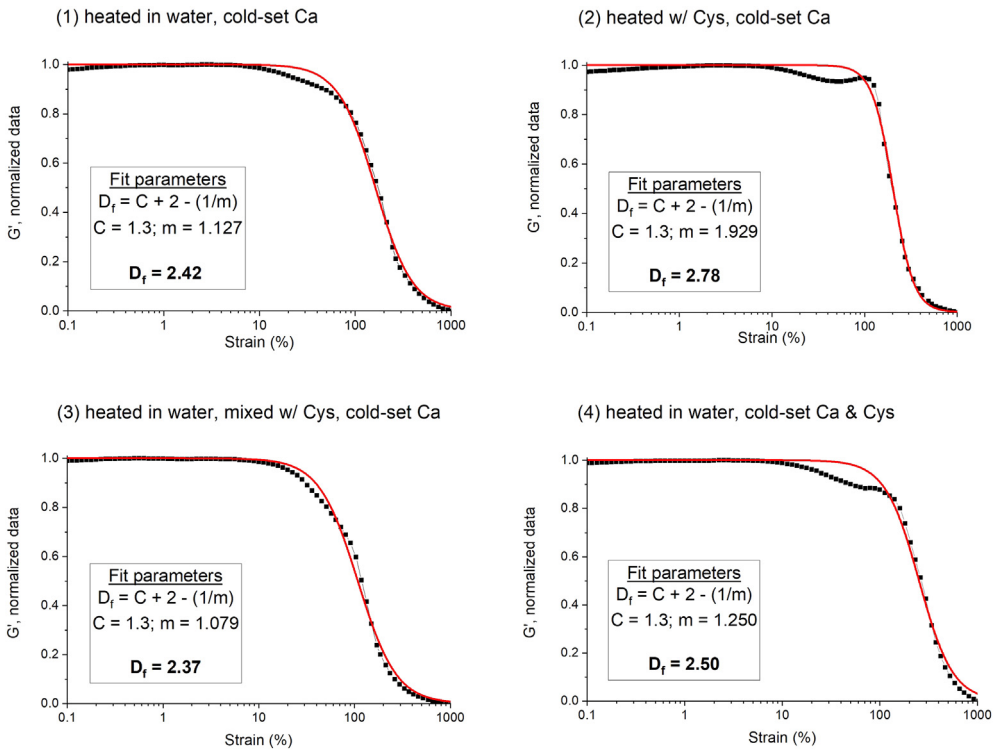

Fig. 6. D_f of the four cold-set WPI gels determined by oscillatory rheology using the "Kraus model". The red line represents the Kraus model on each graph.

The following model is proposed to explain this behavior (Fig. 7). First, the irreversible breaking of β-sheets lowers the modulus at small strains. Then, the aggregates deform and finally, the network is destroyed, and a sharp decrease in modulus is observed at strains about 10–100% (cf. Fig. 6). Since the local conformal changes in the primary particles (i.e., the WPI aggregates) do not change the overall connectivity of the network, we used the Kraus model to describe the breakdown of these whey protein gels at larger strains.

Elasticity inside the "soft" fractals varied depending on the addition of Cys to the gel and the preparation method (cf. Fig. 6). Gel 2 was built from structural units without disulfide bonds, hence, they were able to deform significantly when subjected to high strain amplitudes. Gels 1, 3 and 4 were formed from the same heat-induced aggregates, but had a different fractal structure (cf. AFM images, Fig. 2d, e and 2f respectively) and therefore behaved differently. In gel 4, where less calcium ions were involved in the formation of the network, polymers chains were probably able to rearrange and stretch at high strain amplitudes.

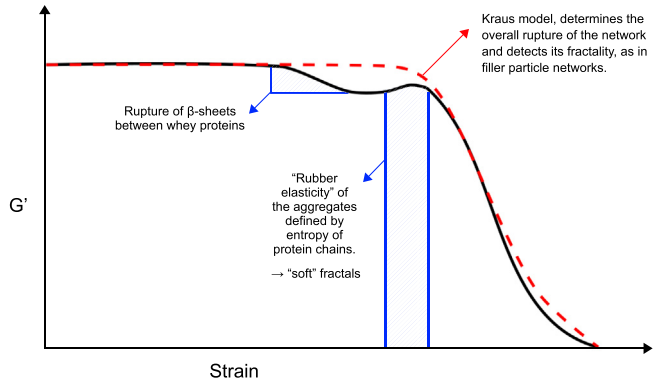

Fig. 7. Hypothetical model of the successive events leading to the rupture of WPI cold-set gels under increasing strain amplitudes.

3.3. Impact of heating on the properties of the cold-set gel

Fig. 8 shows the rheological properties of the WPI cold-set gel (gel 1), before and after heat treatment. According to the amplitude sweeps curves presented in Fig. 8a, the gel still behaved as a viscoelastic gel with dominating elastic properties (i.e., $G'' < G'$) after heat treatment at 90 °C, but its rheological properties were significantly modified by heating. In addition to the significant increase of G', from 2.2 ± 0.6 to 107.1 ± 3.5 kPa, irreversible deformation of the gel occurred at ~0.8% of oscillation strain, against ~15% before heat treatment (Fig. 8a). So, the gel network was not only stiffer, but also more brittle. These results are in line with our previous observations on composite cold-set gels of WPI and potato starch: the pure WPI gel (used as control in the study) was harder and more brittle after heating above 85 °C (Lavoisier and Aguilera, 2019). It is also in accordance with the results of Hongsprabhas and Barbut (1997b), who reported that heating calcium-induced cold-set WPI gels increased the Young's modulus and the shear stress, but reduced the shear strain. Authors suggested that heating may increase interactions (hydrophobic and disulfide bonds) between the protein aggregates of the gels and modify their microstructure. A similar trend has also been observed when increasing the salt concentration used to induce cold gelation: at fracture, the shear stress increased, whilst the shear strain decreased (Bryant and McClements, 1998). Furthermore, a strengthening of the gel was also observed at lower temperatures of heat treatment (Fig. 8b). G'_0 also increased significantly after heat treatment at 50, 60, 70, and 80 °C. Although, this reinforcement increased with temperature (Fig. 8b). Such a rise in G'_0 is probably due to the formation of new hydrophobic interactions and/or disulfide bonds, which are both promoted by temperature (Bryant and McClements, 1998).

To better understand why the rheological properties of the WPI cold-set gel were modified by heat treatment, the thermal properties of gel 1 were measured with DSC (Fig. 9a). An endothermic peak at 71.5 °C was first observed when the gel was heated from 20 to 90 °C. But then, the same endothermic peak appeared when the sample was subjected to heating/cooling cycles between 20 and 90 °C, meaning that this

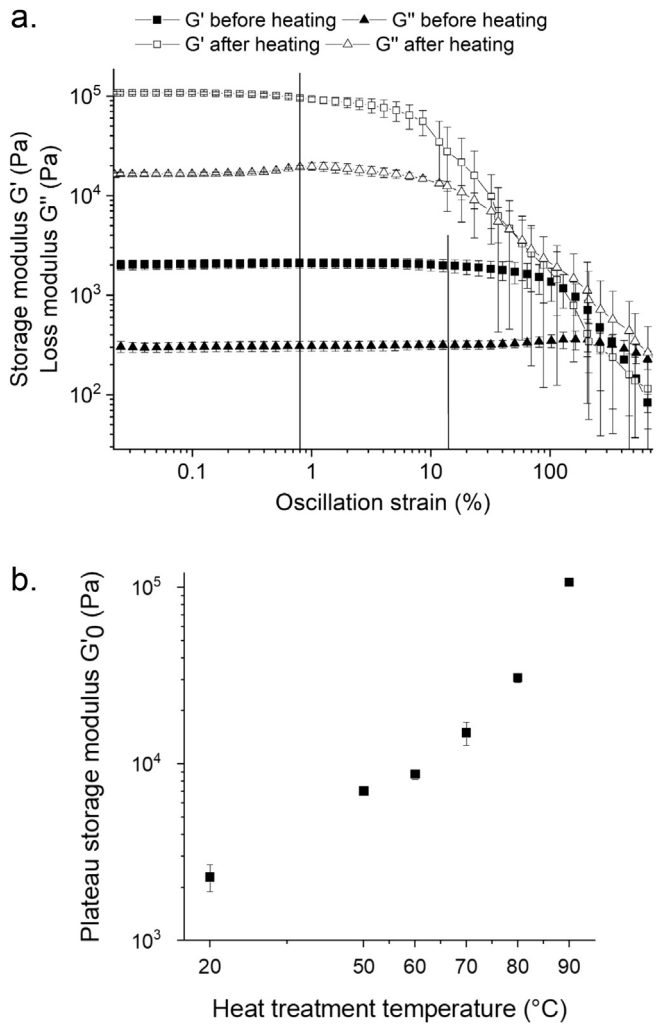

Fig. 8. (a) Amplitude sweep curves of the WPI gel cold-set with calcium (gel 1) at 20°, before and after heat treatment at 90 °C (temperature sweeps); (b) Plateau storage modulus (G'_0) of the WPI gel cold-set with calcium (gel 1) at 20 °C, after heat treatment from 20 to 50, 60, 70, 80 or 90 °C at 1 °C/min (temperature sweeps).

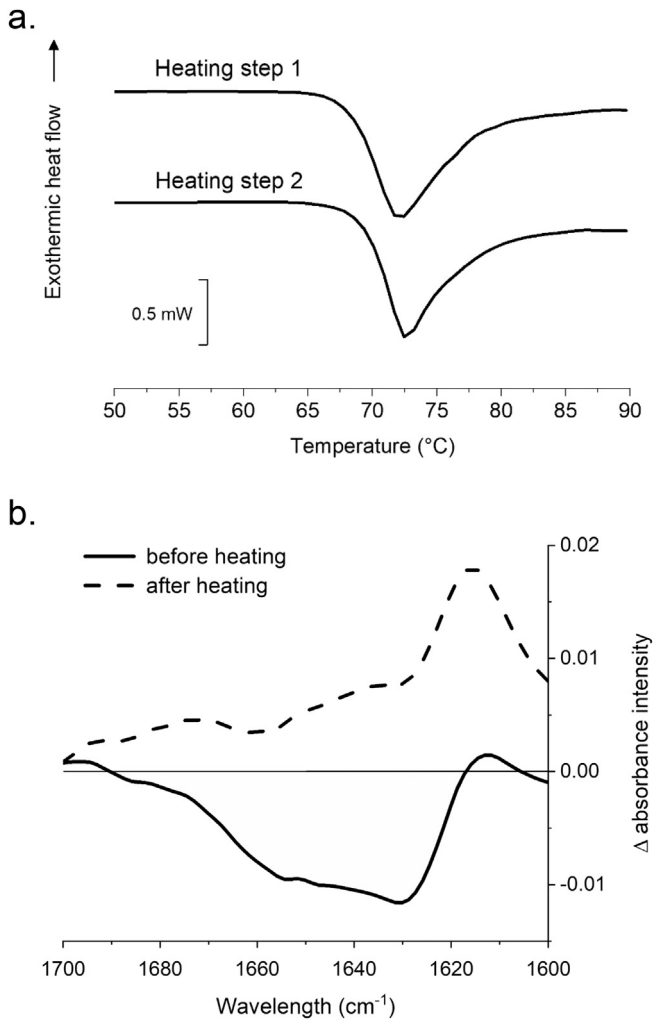

Fig. 9. (a) DSC thermograms for the WPI gel cold-set with calcium (gel 1), heated two consecutive times from 20 to 90 °C at 1 °C/min. To facilitate comparison, the DSC scans were displaced vertically to arbitrary amounts; (b) ATR-FTIR spectroscopy spectra of the WPI gel cold-set with calcium (gel 1), before (solid line) and after (dash line) heating to 90 °C.

transition was reversible to a second heating cycle. The enthalpy change (ΔH) of the transition was 67.3 ± 2.2 J/g. We attributed this reversible thermal transition to the unfolding of the intermolecular hydrogen-bonding β-sheets present in the cold-set gel structure. Indeed, reverse unfolding of β-sheets in proteins has been observed before by calorimetric studies (Wimley and White, 2004).

This hypothesis was supported by the study of the secondary structure of whey proteins in gel 1 by ATR-FTIR spectroscopy, before and after heating to 90 °C (Fig. 9b). The secondary structure of the whey proteins was the same in the heat-induced aggregates and in the calcium-induced gels (cf. Fig. 1). Similar molecular structure of the proteins following heat treatment and within the cold-set gels were also observed by FTIR spectroscopy in β-lg gels induced by ferrous ions (Remondetto and Subirade, 2003) and in soy protein isolate gels induced by calcium ions (Maltais et al., 2008). This observation confirms that the heat-induced aggregates are the structural units of gel 1 and its formation is the result of the association of these structural units. However, an increase in band intensity at 1618 cm^{-1} was observed on the spectrum of the cold-set gel heated to 90 °C (Fig. 9b) meaning that intermolecular interactions, through hydrogen-bonding β-sheets, were enhanced by heating. Furthermore, this spectrum shows an increment in band intensities at ~1640 cm^{-1} and at ~1675 cm^{-1}, wavelengths associated to random coils and turns respectively (Geara, 1999). An increase in random coil conformation reflects a gain in conformational entropy and has been related to unfolding and irreversible aggregation of whey proteins (O'Loughlin et al., 2015). This suggests that heat treatment increased the irreversible unfolding of whey proteins. The molecular conformation of the heat-induced aggregates, the structural units of the cold-set gel, was therefore modified by heating the gel at 90 °C.

3.4. Impact of heating on the microstructure of the cold-set gel

The microstructure of the WPI cold-set gel was observed with CLSM, before and after heating to 90 °C (Fig. 10). CLSM images revealed that the microstructure of the gel became coarser after heat treatment, with denser clusters and larger pores (Fig. 10b). These observations agree with the results of Hongsprabhas and Barbut (1997b) who reported that heating of cold-set WPI gels at 80 °C for 30 min caused some of the protein aggregates to collapse together, leading to a lower degree of connectivity among them.

The microstructure of gel 1 was also studied through cryo-SEM, before and after heat treatment at 90 °C (Fig. 11). Cryo-SEM images confirmed that the WPI cold-set gel was modified by heating. Numerous threads appeared within the pores of the connected protein network (Fig. 11b), suggesting an increase in interactions between the structural units of the gel and an overall change of the microstructure after heat treatment. Some

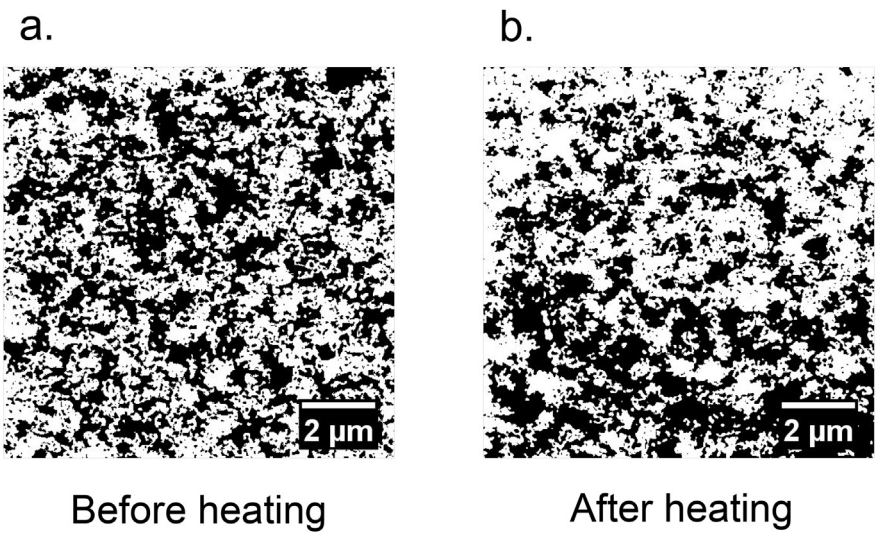

Fig. 10. Images of the WPI gel cold-set with calcium (gel 1), (a) before and (b) after heating to 90 °C. The background appears in black and the WPI network in white.

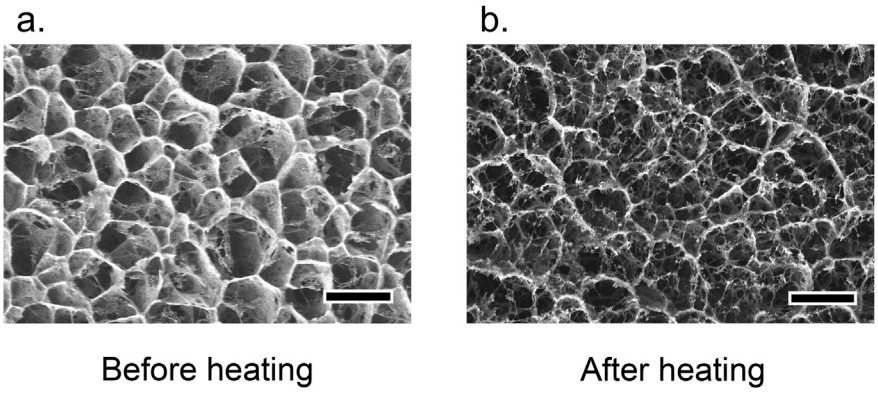

Fig. 11. Images of the WPI gel cold-set with calcium (gel 1), (a) before and (b) after heating to 90 °C. The markers represent 2 μm.

of those threads were stretched and seemed connected on either sides, whereas others looked like a collection of small threads attached to the surface of the particles, resulting in a "hairy" appearance. This structural feature, called "hairiness", has been described before for heat-induced whey protein gels, especially when the NaCl concentration in the system was increased (Langton and Hermansson, 1996). However, cryo-SEM images should be analyzed with caution since even fast freezing of high-moisture samples may lead to artifacts, i.e., hexagonal-shaped contours formed by segregated material (Efthymiou et al., 2017).

3.5. *Effect of cysteine addition on the properties of the cold-set gel after heating*

Changes in the rheological properties of the four WPI cold-set gels were followed by measuring G′ during heating from 20 to 90 °C and cooling back to 20 °C (Fig. 12). G′ increased for all samples during the heating segment and continued to rise throughout the cooling step. However, the three gels that were modified by the addition of Cys reached lower values of G′ at the end of the heat treatment. Differences between the gels appeared mainly during the heating phase of the temperature sweep. The final G′ value for gel 2 was 42.3 ± 8.7 kPa, compared to 93.2 ± 10.1 kPa for gel 1. As discussed before, gel 2 had a more packed network structure (cf. Fig. 5), therefore it probably presented less available sites for new molecular interactions during heating/cooling, resulting in a lower G′. Gel 3 reached a similar final

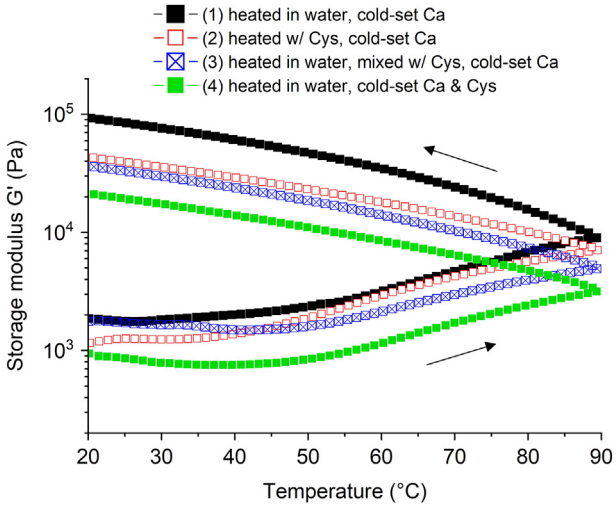

Fig. 12. Temperature sweep curves of the four WPI cold-set gels: (1) WPI heated in water and cold-set with calcium; (2) WPI heated with Cys and cold-set with calcium; (3) WPI heated in water, mixed with Cys, and cold-set with calcium; (4) WPI heated in water, and cold-set with calcium and free Cys together in solution. G″ and error bars are not indicated for the sake of clarity.

G′ (36.5 ± 9.2 kPa) as gel 2, but in this case G′ first decreased slightly up to ~45 °C before increasing steadily as it approached 90 °C. According to the AFM pictures (cf. Fig. 2e, e'), this gel had an open structure, which could explain the decrease in G′ at the beginning of the heat treatment. The network was loose enough to allow movement in its structure as the internal energy of the system increased. Then, the added Cys may have hindered the formation of additional disulfide bonds by blocking some of the thiol groups on the particles of whey proteins, which led to a lower G′. Regarding gel 4, G′ was 21.0 ± 6.6 kPa at the end of the heat treatment, which was the lowest value of all samples. Similar to gel 3, G′ decreased slightly when heated to ~45 °C, reflecting the relatively loose structure of the initial gel. As commented before, complex formation between free Cys and calcium (cf. Fig. 3) reduced the availability of both to interact with the whey protein particles. So, even if some thiol groups may have been blocked by Cys, reduced values of G′ are mainly attributed to the lower ionic strength in the system. This suggests that additional calcium bridges may be involved in the reinforcement of the structure of gel 1. Calcium ions in excess, that did not form electrostatic interactions during cold gelation, may participate in the rearrangement of the whey protein network during heating. Furthermore, G' steadily increased in all samples during the cooling phase of the temperature sweep. This important rise in G′ is probably related to the formation of the intermolecular β-sheets observed with ATR-FTIR and DSC (cf. Fig. 9).

According to these results, it appears that additional disulfide bonds and calcium bridges form during heating ("strong cross-links"), whereas hydrophobic interactions form during cooling ("weak cross-links"), all contributing to an increase in rigidity of the gel and an irreversible modification of the protein network structure.

4. Conclusions

The presence of Cys influenced the cold gelation of whey proteins at pH 7, and this effect depended on the method used. When Cys was added during the first step of cold gelation (i.e., the heating step), it modified heat-induced aggregation of WPI. The unfolding of whey proteins was increased, and aggregates formed through non-covalent interactions. Calcium addition then led to the formation of a dense gel network with a fractal dimension of 2.8. When Cys was added during the second step of cold gelation (i.e., calcium addition at room temperature), the growth of the particle network was different. Highly branched clusters of WPI were observed, and the gel had a fractal dimension of 2.4. However, when Cys and $CaCl_2$ solutions were mixed before adding to the dispersion of WPI aggregates, calcium ions and Cys interacted first, resulting in a reduction of the ionic strength of the solution. Consequently, the formation of clusters was hindered, and the structure of the gel network was altered ($D_f = 2.5$).

The viscoelastic properties and the microstructure of the WPI cold-set gel were irreversibly modified by heating. An increase in intermolecular interactions, especially hydrogen-bonding β-sheets, was observed. The gel was stiffer and more brittle after heat treatment, and its microstructure was coarser. These changes should be taken into account when designing soft foods based on cold-set globular protein gels, especially if they undergo thermal treatments or are used in cooking.

Modification of the WPI cold-set gel with Cys was determinant to understand the phenomena occurring at the molecular level during heat treatment. The study of the rheological properties of these modified gels showed that new disulfide bonds and new calcium bridges formed in the WPI cold-set gel during heating. These "strong cross-links" added to the hydrophobic interactions formed during cooling ("weak cross-links") and contributed to the increase in rigidity of the model gel.

Since free Cys and heating influence the properties of WPI cold-set gels, different thermal treatments, in combination with the addition of Cys, could be used to obtain a range of textures and mouthfeel.

Conflict of interest

The authors declare that they have no conflict of interest.

Acknowledgments

This work was supported by CONICYT (the National Commission for Science and Technology, Chile) through FONDECYT project no. 1150395, FONDEQUIP project EQ M170120, and is part of the doctoral thesis of Anaïs Lavoisier also under support of CONICYT, doctoral fellowship no. 21160413. The authors would like to thank Ingo Lieberwirth and Gunnar Glaβer for cryo-SEM imaging, Rüdiger Berger and Uwe Rietzler for support with the AFM as well as Kaloian Koynov, Andreas Hanewald and Andreas Best for CLSM imaging and technical support with rheological measurements. Author Aguilera acknowledges financial support for work on soft gels by the Korea Food Research Institute (KFRI).

References

Aguilera, J.M., 1995. Gelation of whey proteins. Food Technol. 49, 83–89.
Ako, K., Durand, D., Nicolai, T., Becu, L., 2009. Quantitative analysis of confocal laser scanning microscopy images of heat-set globular protein gels. Food Hydrocolloids 23, 1111–1119. https://doi.org/10.1016/j.foodhyd.2008.09.003.
Alting, A.C., De Jongh, H.H.J., Visschers, R.W., Simons, J.W.F.A., 2002. Physical and chemical interactions in cold gelation of food proteins. J. Agric. Food Chem. 50, 4682–4689. https://doi.org/10.1021/jf011657m.
Alting, A.C., Hamer, R.J., De Kruif, C.G., Visschers, R.W., 2003. Cold-set globular protein gels: interactions, structure and rheology as a function of protein concentration. J. Agric. Food Chem. 51, 3150–3156. https://doi.org/10.1021/jf0209342.
Andoyo, R., Lestari, V.D., Mardawati, E., Nurhadi, B., 2018. Fractal dimension analysis of texture formation of whey protein-based foods. Int. J. Food Sci. 2018, 1–17. https://doi.org/10.1155/2018/7673259.
Baussay, K., Le Bon, C., Nicolai, T., Durand, D., Busnel, J.P., 2004. Influence of the ionic strength on the heat-induced aggregation of the globular protein β-lactoglobulin at pH 7. Int. J. Biol. Macromol. 34, 21–28. https://doi.org/10.1016/j.ijbiomac.2003.11.003.
Brodkorb, A., Croguennec, T., Bouhallab, S., Kehoein, J.J., 2016. Heat-induced denaturation, aggregation and gelation of whey proteins. In: McSweeney, P., O'Mahony, J.A. (Eds.), Advanced Dairy Chemistry, Volume 1B: Proteins: Applied Aspects. Springer, New York, pp. 155–178.
Bryant, C.M., McClements, D.J., 1998. Molecular basis of protein functionality with special consideration of cold-set gels derived from hat-denatured whey. Trends Food Sci. Technol. 9, 143–151. https://doi.org/10.1016/S0924-2244(98)00031-4.
Bryant, C.M., McClements, D.J., 2000. Influence of NaCl and CaCl2 on cold-set gelation of heat-denatured whey protein. Food Chem. Toxicol. 65, 801–804.
Cheison, S.C., Kulozik, U., 2017. Impact of the environmental conditions and substrate pre-treatment on whey protein hydrolysis: a review. Crit. Rev. Food Sci. Nutr. 57, 418–453. https://doi.org/10.1080/10408398.2014.959115.
Dan, Z., Labuza, T.P., 2010. Effect of cysteine on lowering protein aggregation and subsequent hardening of whey protein isolate (WPI) protein bars in WPI/buffer model systems. J. Agric. Food Chem. 58, 7970–7979. https://doi.org/10.1021/jf100743z.
Durand, D., Gimel, J.C., Nicolai, T., 2002. Aggregation, gelation and phase separation of heat denatured globular proteins. Phys. A 304, 253–265. https://doi.org/10.1016/S0378-4371(01)00514-3.
Efthymiou, C., Williams, M.A.K., Mcgrath, K.M., 2017. Revealing the structure of high-water content biopolymer networks : diminishing freezing artefacts in cryo-SEM images. Food Hydrocolloids 73, 203–212. https://doi.org/10.1016/j.foodhyd.2017.06.040.
Elkhalifa, A.E.O., El-Tinay, A.H., 2002. Effect of cysteine on bakery products from wheat – sorghum blends. Food Chem. 77, 133–137.
Elofsson, C., Dejmek, P., Paulsson, M., Burling, H., 1997. Atomic force microscopy studies on whey proteins. Int. Dairy J. 7, 813–819. https://doi.org/10.1016/S0958-6946(98)00008-9.
Geara, C., 1999. Study of the Gelation of Whey Protein Isolate by FTIR Spectroscopy and Rheological Measurements. McGill University, Montreal, Canada. https://doi.org/10.16953/deusbed.74839.
Grewal, M.K., Huppertz, T., Vasiljevic, T., 2018. FTIR fingerprinting of structural changes of milk proteins induced by heat treatment, deamidation and dephosphorylation. Food Hydrocolloids 80, 160–167. https://doi.org/10.1016/j.foodhyd.2018.02.010.
Havea, P., Singh, H., Creamer, L.K., 2001. Characterization of heat-induced aggregates of B-lactoglobulin, A-lactalbumin and bovine serum albumin in a whey protein concentrate environment. J. Dairy Res. 68, 483–497.
Havea, P., Watkinson, P., Kuhn-Sherlock, B., 2009. Heat-induced whey protein gels: protein-protein interactions and functional properties. J. Agric. Food Chem. 57, 1506–1512. https://doi.org/10.1021/jf802559z.
Hines, M.E., Foegeding, E.A., 1993. Interactions of α-lactalbumin and bovine serum albumin with β-lactoglobulin in thermally induced gelation. J. Agric. Food Chem. 41, 341–346. https://doi.org/10.1021/jf00027a001.

Hoffmann, M.A.M., Van Mil, P.J.J.M., 1997. Heat-induced aggregation of β-lactoglobulin: role of the free thiol group and disulfide bonds. J. Agric. Food Chem. 45, 2942–2948. https://doi.org/10.1021/jf960789q.
Hongsprabhas, P., 1997. Mechanisms of Calcium-Induced Cold Gelation of Whey Protein Isolate. Univ. Guelph, Ottawa, Canada.
Hongsprabhas, P., Barbut, S., 1997. Ca2+-Induced cold gelation of whey protein isolate: effect of two-stage gelation. Food Res. Int. 30, 523–527. https://doi.org/10.1016/S0963-9969(98)00010-6.
Hongsprabhas, P., Barbut, S., 1997. Effect of gelation temperature on Ca2+-induced gelation of whey protein isolate. LWT - Food Sci. Technol. 30, 45–49.
Hongsprabhas, P., Barbut, S., Marangoni, A.G., 1999. The structure of cold-set whey protein isolate gels prepared with Ca++. Lebensm.-Wiss. u.-Technol. 32, 196–202.
Huggins, C., Tapley, D.F., Jensen, E.V., 1951. Sulphydryl-disulphide relationships in the induction of gels in proteins by urea. Nature 167, 592–593. https://doi.org/10.1038/351111a0.
Ikeda, S., Morris, V.J., 2002. Fine-stranded and particulate aggregates of heat-denatured whey proteins visualized by atomic force microscopy. Biomacromolecules 3, 382–389. https://doi.org/10.1021/bm0156429.
Joshi, B., Beccard, S., Vilgis, T.A., 2008. Fractals in crystallizing food systems. Curr. Opin. Food Sci. 21, 39–45. https://doi.org/10.1016/j.cofs.2018.05.009.
Jung, J.M., Savin, G., Pouzot, M., Schmitt, C., Mezzenga, R., 2008. Structure of heat-induced β-lactoglobulin aggregates and their complexes with sodium-dodecyl sulfate. Biomacromolecules 9, 2477–2486. https://doi.org/10.1021/bm800502j.
Kehoe, J.J., Wang, L., Morris, E.R., Brodkorb, A., 2011. Formation of non-native β-lactoglobulin during heat-induced denaturation. Food Biophys. 6, 487–496. https://doi.org/10.1007/s11483-011-9230-3.
Kharlamova, A., Nicolai, T., Chassenieux, C., 2018. Calcium-induced gelation of whey protein aggregates: kinetics, structure and rheological properties. Food Hydrocolloids 79, 145–157. https://doi.org/10.1016/j.foodhyd.2017.11.049.
Kharlamova, A., Chassenieux, C., Nicolai, T., 2018. Acid-induced gelation of whey protein aggregates: kinetics, gel structure and rheological properties. Food Hydrocolloids 81, 263–272. https://doi.org/10.1016/j.foodhyd.2018.02.043.
Kuhn, K.R., Cavallieri, Â.L.F., da Cunha, R.L., 2010. Cold-set whey protein gels induced by calcium or sodium salt addition. Int. J. Food Sci. Technol. 45, 348–357. https://doi.org/10.1111/j.1365-2621.2009.02145.x.
Langton, M., Hermansson, A., 1996. Image analysis of particulate whey protein gels. Food Hydrocolloids 10, 179–191. https://doi.org/10.1016/S0268-005X(96)80033-6.
Lavoisier, A., Aguilera, J.M., 2019. Starch gelatinization inside a whey protein gel formed by cold gelation. J. Food Eng. 256, 18–27. https://doi.org/10.1016/j.jfoodeng.2019.03.013.
Lefèvre, T., Subirade, M., 1999. Structural and interaction properties of β-lactoglobulin as studied by FTIR spectroscopy. Int. J. Food Sci. Technol. 34, 419–428. https://doi.org/10.1046/j.1365-2621.1999.00311.x.
Mahmoudi, N., Mehalebi, S., Nicolai, T., Durand, D., Riaublanc, A., 2007. Light-scattering study of the structure of aggregates and gels formed by heat-denatured whey protein isolate and β-lactoglobulin at neutral pH. J. Agric. Food Chem. 55, 3104–3111. https://doi.org/10.1021/jf063029g.
Majzoobi, M., Farahnaky, A., Jamalian, J., Radi, M., 2011. Effects of L-Cysteine on some characteristics of wheat starch. Food Chem. 124, 795–800. https://doi.org/10.1016/j.foodchem.2010.06.098.
Maltais, A., Remondetto, G.E., Subirade, M., 2008. Mechanisms involved in the formation and structure of soya protein cold-set gels: a molecular and supramolecular investigation. Food Hydrocolloids 22, 550–559. https://doi.org/10.1016/j.foodhyd.2007.01.026.
Marangoni, A.G., Barbut, S., McGauley, S.E., Marcone, M., Narine, S.S., 2000. On the structure of particulate gels - the case of salt-induced cold gelation of heat-denatured whey protein isolate. Food Hydrocolloids 14, 61–74. https://doi.org/10.1016/S0268-005X(99)00046-6.
Nečas, D., Klapetek, P., 2012. Gwyddion: an open-source software for SPM data analysis. Cent. Eur. J. Phys. 10, 181–188. https://doi.org/10.2478/s11534-011-0096-2.
Nguyen, N.H.A., Wong, M., Guyomarc'h, F., Havea, P., Anema, S.G., 2014. Effects of non-covalent interactions between the milk proteins on the rheological properties of acid gels. Int. Dairy J. 37, 57–63. https://doi.org/10.1016/j.idairyj.2014.03.001.
Nicolai, T., Durand, D., 2013. Controlled food protein aggregation for new functionality. Curr. Opin. Colloid Interface Sci. 18, 249–256. https://doi.org/10.1016/j.cocis.2013.03.001.
Ong, L., Dagastine, R.R., Kentish, S.E., Gras, S.L., 2011. Microstructure of milk gel and cheese curd observed using cryo scanning electron microscopy and confocal microscopy. LWT - Food Sci. Technol. 44, 1291–1302. https://doi.org/10.1016/j.lwt.2010.12.026.
O'Loughlin, I.B., Kelly, P.M., Murray, B.A., Fitzgerald, R.J., Brodkorb, A., 2015. Concentrated whey protein ingredients: a Fourier transformed infrared spectroscopy investigation of thermally induced denaturation. Int. J. Dairy Technol. 68, 349–356. https://doi.org/10.1111/1471-0307.12239.
PSAAE (Purdue School of Aeronautics and Astronautics Engineering), 1998. Heats of Formation and Chemical Compositions. Purdue University. https://engineering.purdue.edu/~propulsi/propulsion/comb/propellants.html. (Accessed 15 July 2019).
Rao, M.A., 2007. Rheology of Fluids and Semisolid Foods Principles and Applications, second ed. Springer, Geneva, New York.
Remondetto, G.E., Subirade, M., 2003. Molecular mechanisms of Fe2+-induced β-lactoglobulin cold gelation. Biopolymers 69, 461–469. https://doi.org/10.1002/bip.10423.
Roff, C.F., Foegeding, E.A., 1996. Dicationic-induced gelation of pre-denatured whey protein isolate. Food Hydrocolloids 10, 193–198. https://doi.org/10.1016/S0268-005X(96)80034-8.
Schindelin, J., Arganda-Carreras, I., Frise, E., 2012. Fiji: an open-source platform for biological-image analysis. Nat. Methods 9, 676–682. https://doi.org/10.1038/nmeth.2019.
Schmidt, R.H., Illingworth, B.L., Ahmed, E.M., 1978. Heat-induced gelation of peanut protein/whey protein blends. J. Food Sci. 43, 613–615.
Schmidt, R.H., Illingworth, B.L., Deng, J.C., Cornel, J.A., 1979. Multiple regression and response surface analysis of the effects of calcium chloride and cysteine on heat-induced whey protein gelation, 27, 529–532.
Schneider, C.A., Rasband, W.S., Eliceiri, K.W., 2012. NIH Image to ImageJ: 25 years of image analysis. Nat. Methods 9, 671–675. https://doi.org/10.1038/nmeth.2089.
Shih, W.H., Shih, W.Y., Kim, S.I.l., Liu, J., Aksay, I.A., 1990. Scaling behavior of the elastic properties of colloidal gels. Phys. Rev. A. 42, 4772–4779. https://doi.org/10.1103/PhysRevA.42.4772.
Smithers, G.W., 2015. Whey-ing up the options - yesterday, today and tomorrow. Int. Dairy J. 48, 2–14. https://doi.org/10.1016/j.idairyj.2015.01.011.
The UniProt Consortium, 2019. UniProt: a worldwide hub of protein knowledge. Nucleic Acids Res. 47, D506–D515. https://doi.org/10.1093/nar/gky1049.
Vilgis, T.A., Heinrich, G., Klüppel, M., 2009. Reinforcement of Polymer Nano-Composites: Theory, Experiments and Applications. Cambridge University Press, Cambridge.
Vreeker, R., Hoekstra, L.L., den Boer, D.C., Agterof, W.G.M., 1992. Fractal aggregation of whey proteins. Food Hydrocolloids 6, 423–435. https://doi.org/10.1016/S0268-005X(09)80028-3.
Walstra, P., van Vliet, T., Bremer, L.G.B., 1991. On the fractal nature of particle gels. In: Dickinson, E. (Ed.), Food Polymers, Gels and Colloids. Woodhead Publishing, Cambridge, pp. 369–382. https://doi.org/10.1533/9781845698331.369.
Wang, C.H., Damodaran, S., 1990. Thermal gelation of globular proteins: weight-average molecular weight dependence of gel strength. J. Agric. Food Chem. 38, 1157–1164. https://doi.org/10.1021/jf00095a001.
Wijayanti, H.B., Oh, H.E., Sharma, R., Deeth, H.C., 2013. Reduction of aggregation of β-lactoglobulin during heating by dihydrolipoic acid. J. Dairy Res. 80, 383–389. https://doi.org/10.1017/S0022029913000332.
Wijayanti, H.B., Bansal, N., Sharma, R., Deeth, H.C., 2014. Effect of sulphydryl reagents on the heat stability of whey protein isolate. Food Chem. 163, 129–135. https://doi.org/10.1016/j.foodchem.2014.04.094.
Wimley, W.C., White, S.H., 2004. Reversible unfolding of β-sheets in membranes: a calorimetric study. J. Mol. Biol. 342, 703–711. https://doi.org/10.1016/j.jmb.2004.06.093.
Wu, H., Xie, J., Morbidelli, M., 2005. Kinetics of cold-set diffusion-limited aggregations of denatured whey protein isolate colloids. Biomacromolecules 6, 3189–3197. https://doi.org/10.1021/bm050532d.